Original paper

Modelling of the refining space working under reduced pressure

Jaroslav Kloužek and Lubomír Němec

Laboratory of Inorganic Materials, Institute of Inorganic Chemistry ASCR and the Institute of Chemical Technology, Prague (Czech Republic)

Jiří Ullrich

Glass Service Ltd., Vsetín (Czech Republic)

The refining channel working under reduced pressure and at medium temperatures was modelled experimentally and mathematically. The bubble growth rate was measured in the temperature interval 1200 to 1450 °C and pressures 15 to 50 kPa for the lead glass melt with and without refining agent. The bubble nucleation temperature was determined and the glass foam on the level was observed using high-temperature observation, video recording and image analysis. The temperature–pressure areas were defined in which the bubble nucleation and glass foaming did not interfere with efficient refining. The simplified mathematical model of bubble growth or dissolution under nonisothermal conditions was formulated and applied to the mathematical modelling of glass melt and bubble behaviour in the refining channel. Having applied the critical bubble pathways, the pull rates of the modelled channel have been calculated in the experimentally examined area of admissible temperatures and pressures. Besides temperature, the reduced pressure proved to be an efficient refining factor; the temperature increase by 35 K corresponded to the pressure decrease by about 10 kPa under given conditions. The results were discussed with respect to simplified relations between refining efficiency and temperature or pressure. The combination of experimental and mathematical modelling showed to be a sufficient and reliable tool for acquiring the fundamental parameters of the process under real melting conditions.

Modellierung der unter vermindertem Druck arbeitenden Läuterzone

Der unter vermindertem Druck und bei mittleren Temperaturen arbeitende Läuterkanal wurde experimentell und mathematisch modelliert. Die Wachstumsrate der Blasen in einer Bleiglasschmelze mit oder ohne Läutermittel wurde im Temperaturbereich von 1200 bis 1450 °C und bei Drücken von 15 bis 50 kPa gemessen. Die Blasenbildungs-Temperatur wurde bestimmt, und der Schaum auf der Glasbadoberfläche wurde mittels Hochtemperatur-Kamera, Videorekorder und Bildanalyse beobachtet. Es wurden die Temperatur-Druck-Gebiete bestimmt, in denen Blasenbildung und Glasschaum einer wirkungsvollen Läuterung nicht entgegenstanden. Ein vereinfachtes mathematisches Modell des Blasenwachstums oder der Blasenauflösung unter nichtisothermen Bedingungen wurde formuliert und für die mathematische Modellierung von Glasschmelze und Blasenverhalten im Läuterkanal verwendet. Unter Einbeziehung des kritischen Blasenaufstiegs wurden die Durchsatzraten des modellierten Kanals für den experimentell untersuchten Temperatur- und Druckbereich berechnet. Neben der Temperatur erwies sich der verminderte Druck als wirkungsvoller Läuterfaktor. Der Anstieg der Temperatur um 35 K stimmte unter den gegebenen Bedingungen mit der Verminderung des Drucks um ungefähr 10 kPa überein. Die Ergebnisse wurden im Hinblick auf die vereinfachten Beziehungen zwischen Läutergrad und Temperatur oder Druck diskutiert. Die Kombination von experimentellem und mathematischem Modell erwies sich als zufriedenstellende und verläßliche Methode, die Prozeßparameter unter realen Schmelzbedingungen zu erhalten.

1. Introduction

Two mechanisms can significantly accelerate the glass fining process – the bubble growth and bubble dissolution by gas diffusion out or into the glass melt. However, only the former mechanism has technological significance, as the complete bubble dissolution is difficult for multicomponent bubbles. The driving force of multicomponent bubble growth in a glass melt is given by the sum of differences between internal partial pressures of single gases in the melt and in the bubble, i.e.:

$$\frac{\mathrm{d}a}{\mathrm{d}\tau} \propto \sum_{i=1}^{n} p_{i\,\mathrm{melt}} - \sum_{i=1}^{n} p_i \,, \tag{1}$$

where a is the bubble radius, τ the time, $p_{i\,\mathrm{melt}}$ the internal partial pressure of the i-th gas dissolved in the melt and p_i its partial pressure in the bubble. The external pressure drop increases the right side of equation (1)

Received 28 October 1999, revised manuscript 30 June 2000.

as the value of $\sum_{i=1}^{n} p_i$ decreases and therefore the fining process at reduced pressure seems to be promising [1]. Two problems are faced when applying the refining under reduced pressure: the construction problems due to glass flow into or out of the fining chamber, and the participation of other processes producing gas phase under reduced pressure, namely glass foaming and bubble nucleation in the melt. In addition, the industrial application of reduced pressure needs modelling of bubble behaviour to find the proper dimensions of the chamber. This fact leads to the laborious measurements of the bubble model data such as gas concentrations, solubilities, diffusion coefficients etc. While the construction problems were solved using siphons [2] or by application of plungers and screwpumps [3], the question of simple bubble modelling and participation of other processes, i.e. bubble nucleation and glass foaming, is usually almost neglected.

The goal of this work is to present a simple way to model bubble behaviour in the refining chamber, to estimate the role of bubble nucleation and glass foaming under reduced pressure conditions and to model the fining efficiency of a low-pressure channel using the obtained laboratory data.

2. Experimental

The bubble growth or dissolution rates can be applied to follow the bubble rising in a fining space. The method of high-temperature bubble observation and subsequent image analysis was used for this purpose [4]. The measurements were performed at constant temperature to obtain the stationary bubble growth rates (i.e. the bubble growth rates after attaining the constant bubble composition). Lead-silica glass containing 20.6 wt% PbO was used in all experiments.

In a typical experiment, the silica-glass observation cell with glass batch was inserted into the chamber furnace to melt up to the fining stage. Subsequently, the chamber pressure was lowered to the required value and the processes of bubble evolution, growth, bubble rising as well as bubble bursting on the glass level were observed and video-recorded. When measuring the bubble growth rates, the size development of 10 to 15 bubbles was examined in each experiment to get an average value. The heterogeneous bubble nucleation and growth was examined using the same method and bubbles arisen on the PtRh wire were observed under temperature increase of 2 K/min; the PtRh sheets were assumed to be the material of the fining chamber walls. The temperature of bubble nucleation was found by extrapolating the bubble radius value to zero. Figures 1a to d show a typical structure of fining bubbles at 1200 °C and pressures between 100 and 15 kPa.

3. Semiempirical model of bubble behaviour

The presented model is based on the following assumptions:

a) The bubble growth rates under nonisothermal conditions and in the later stages of refining consist of two components:
   - the rate of growth corresponding to the diffusion of present gases in the bubble under condition of constant bubble composition, $(da/d\tau)_D$ (this value can be measured by bubble observation at constant temperature);
   - the rate of growth caused by the change of equilibrium and kinetic behaviour of the refining gas when varying temperature, $(da/d\tau)_C$.

b) Both bubble growth components are considered additive:

$$\frac{da}{d\tau} = \left(\frac{da}{d\tau}\right)_D + \left(\frac{da}{d\tau}\right)_C . \tag{2}$$

The values of $(da/d\tau)_D$ can be measured as was already mentioned and they show steep exponential increase with temperature. To obtain the value of $(da/d\tau)_C$, the dependence between the stationary concentration of the refining gas in a bubble and temperature during the stationary period is needed. When applying a suitable empirical function, the probable dependence has the form:

$$C \equiv 50 + \frac{100}{\pi} \operatorname{arctg}\left(\frac{T - T_{50}}{10}\right), \tag{3}$$

where C is the final refining gas concentration in the bubble (in vol.%) at temperature T, and T_{50} the temperature corresponding to the 50 vol.% concentration of the refining gas in the bubble. The value of T_{50} can be experimentally acquired by measuring the bubble partial absorption after abrupt temperature decrease from the given value to temperatures between 1100 and 1200 °C. The volume of a bubble is given by:

$$\frac{4}{3}\pi a^3 = \frac{4}{3}\pi a^3 \frac{C}{100} + V_0 \tag{4}$$

where V_0 is volume fraction of nonrefining gases, e.g. CO_2, N_2 and argon. After rearranging and deriving, we get:

$$\left(\frac{da}{d\tau}\right)_C = \frac{a}{300-3C}\frac{dC}{d\tau} . \tag{5}$$

The derivative $dC/d\tau$ is then obtainable from equation (3) and from the time-temperature history of a bubble, $dT/d\tau$, in a refining chamber:

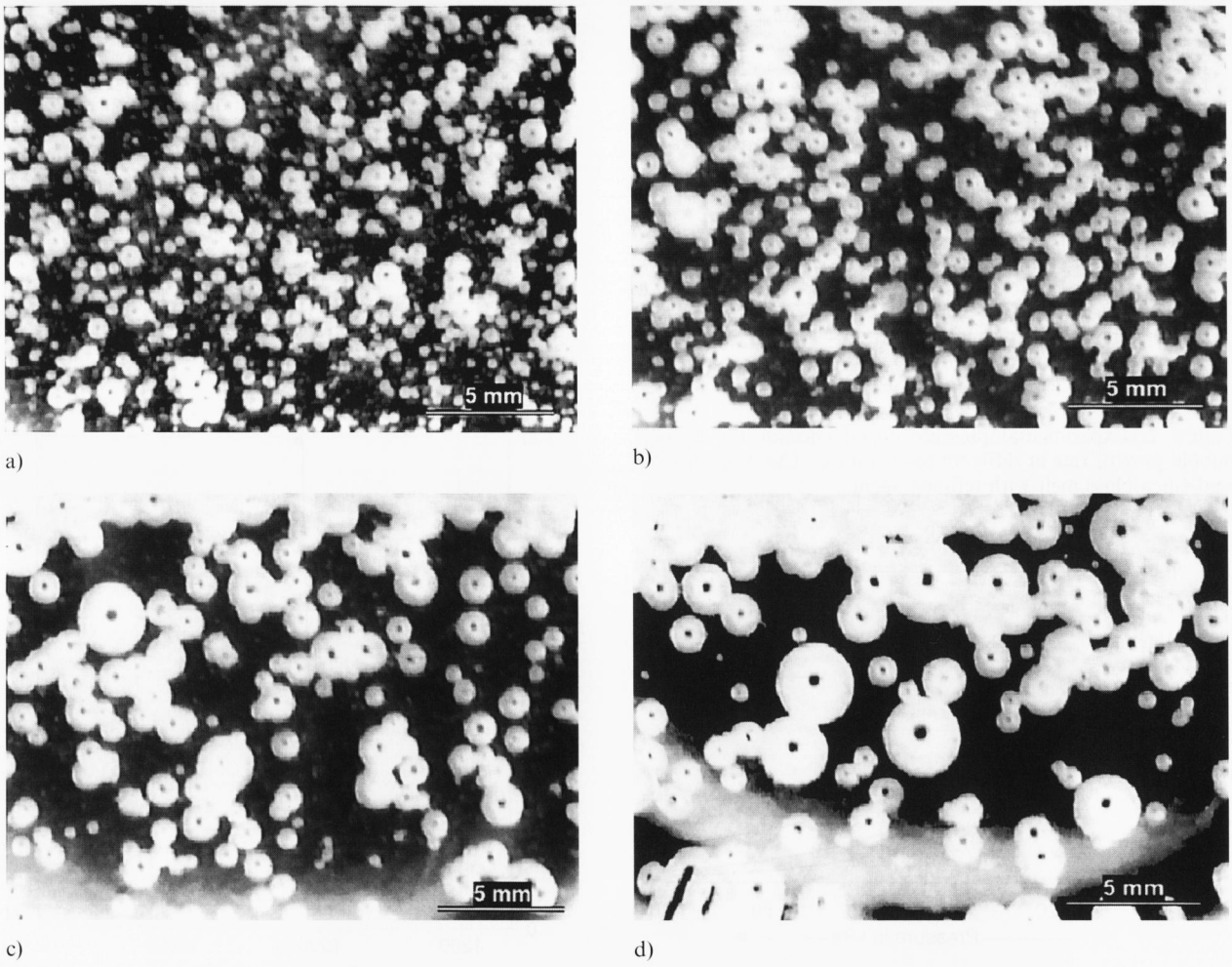

a) b) c) d)

Figures 1a to d. Optical micrographs of bubble distribution in the lead-silica glass melt at 1200 °C and pressures a) 100 kPa, b) 50 kPa, c) 25 kPa and d) 15 kPa, respectively, 5 min after the pressure drop.

$$\frac{dC}{d\tau} = \frac{dC}{dT}\frac{dT}{d\tau}. \qquad (6)$$

The glass model and an iterative procedure were applied to provide equation (6) with the bubble history, $dT/d\tau$ [5], and to follow the bubble pathway.

4. Results of experiments

Two sets of experiments were performed to measure the bubble growth rates at constant temperature, $(da/d\tau)_D$: with glass containing 0.3 wt% of Sb_2O_3 with KNO_3 as a refining agent and with glass without any refining agent. The values of average bubble growth rates, dependent on pressure and temperature, are plotted in figures 2 and 3: The value of T_{50} for the glass with the refining agent at normal pressure was 1623 K; nevertheless when modelling the glass with and without any refining agent, the term $(da/d\tau)_C$ in equation (2) could be neglected in the examined glass melt due to small influence of temperature on the bubble composition.

The glass level recording during observations provided qualitative information about foam arising and foam stability under given conditions. Figure 4 displays a typical picture. Regardless of pressure and presence of the refining agent, the stable foam layer arose only at temperatures lower than 1200 °C.

In the set of experiments examining the bubble nucleation on the PtRh wire, the bubble nucleation temperature was determined. While almost no bubble nucleation was found below 1400 °C and pressures between 6 to 100 kPa in the glass without any refining agent, the values of bubble nucleation temperature in the glass melt containing refining agent and at pressures between 15 and 100 kPa were in a relatively narrow region around 1300 °C. The experimental values of bubble nucleation temperature are presented in table 1.

The appropriate values of temperatures and pressures, resulting from the previous experiments, should be

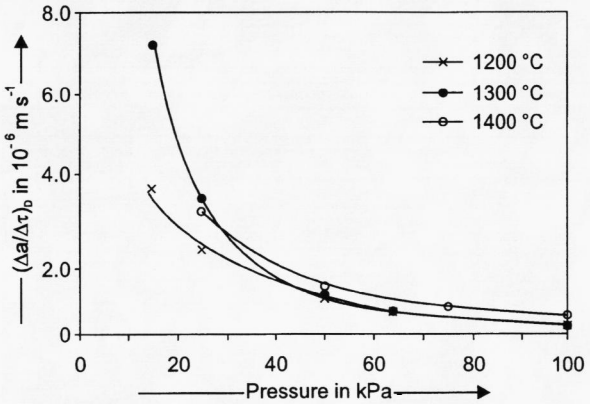

Figure 2. Experimental pressure dependence of the average bubble growth rate at different temperatures, $(\Delta a/\Delta\tau)_D$, for the lead-silica glass melt with refining agent.

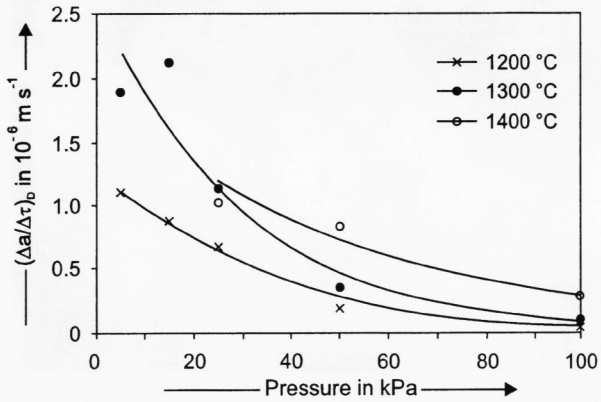

Figure 3. Experimental pressure dependence of the average bubble growth rate at different temperatures, $(\Delta a/\Delta\tau)_D$, for the lead-silica glass melt without refining agent.

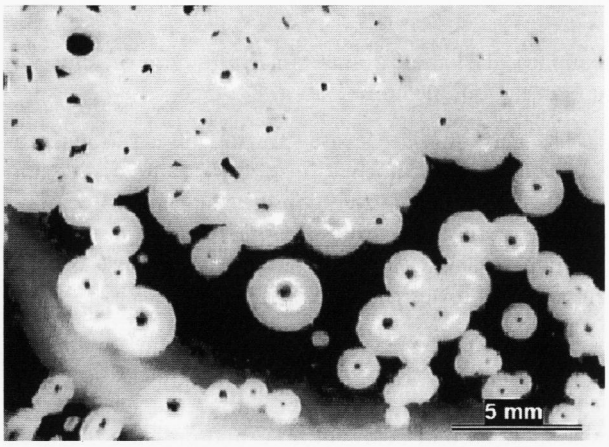

Figure 4. Optical micrograph of the lead-silica glass level in the silica glass cell during refining under reduced pressure at temperature 1200 °C and a pressure of 15 kPa.

Table 1. Values of the bubble nucleation temperatures obtained from the observation of the bubble nucleation on the PtRh wire

	bubble nucleation temperature in °C	
pressure in kPa	glass with refining agent	glass without refining agent
100	1309 ± 13	1490 ± 30
75	1268 ± 13	not measured
50	1312 ± 13	1455 ± 30
25	1295 ± 13	1440 ± 29
15	not measured	1360 ± 27

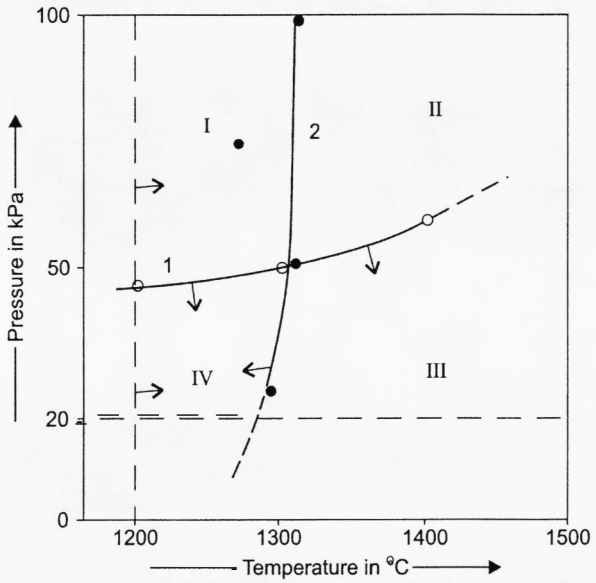

Figure 5. Definition of the temperature–pressure area, applicable to the refining of the lead-silica glass melt containing refining agent; -----: the temperature of the stable foam on the glass level, ○: the curve defining the bubble growth rate $\Delta a/\Delta\tau = 10^{-6}$ m s^{-1}, ●: the curve defining the bubble nucleation temperature.

applied which provide efficient refining and avoid both bubble nucleation and stable foam. As it is obvious from previous fining experiments [1], the values of bubble growth rates higher than about 10^{-6} m s^{-1} ensure rapid refining. The lowest temperature avoiding glass foaming shows to be 1200 °C. Finally, the area of appropriate refining temperatures and pressures is limited by nucleation temperatures. Thus, the areas of acceptable fining temperatures and pressures for both glasses are defined in figures 5 to 6. Here curve 1 designates the couples of temperature and pressure, providing the bubble growth rate 10^{-6} m s^{-1}. The area of bubble growth rates higher then 10^{-6} m s^{-1} is below curve 1. Curve 2 presents the nucleation temperatures and pressures (see table 1), the area without bubble nucleation being on the left side. As for glass foaming, the area of acceptable temperature and pressures is on the right of the estimated temperature 1200 °C (dashed line). The pressure 20 kPa was chosen as lower limit with respect to technical problems in practice. Only a part of temperature and pressure area, designated by number IV, is therefore ap-

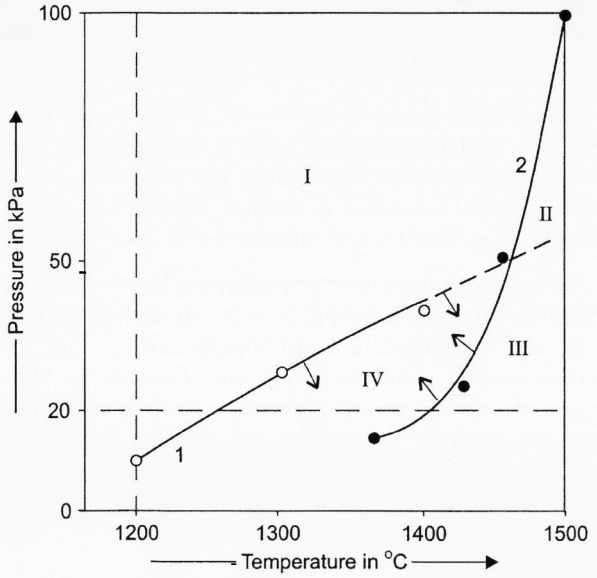

Figure 6. Definition of the temperature–pressure area, applicable to the refining of the lead-silica glass melt without any refining agent; -----: the temperature of the stable foam on the glass level, ○: curve 1 defining the bubble growth rate $\Delta a/\Delta\tau = 10^{-6}$ m s^{-1}, ●: curve 2 defining the bubble nucleation temperature.

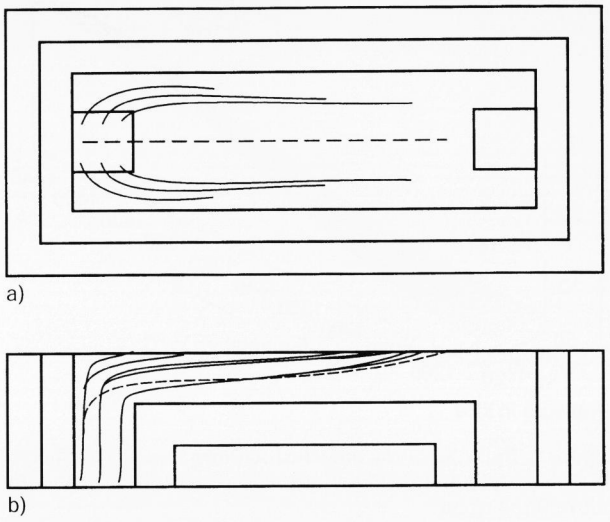

Figures 7a and b. Determination of the critical bubble pathway (– – –) through the refining channel at 1200 °C and a pressure of 30 kPa for the glass melt with refining agent and a pull rate of 10 t/d; a) top view, b) side view.

plicable for the fining and for the mathematical modelling of the fining chamber.

5. Results of mathematical modelling

The basic refining space used in these calculations was a channel 1160 mm long and 400 mm wide, having the glass layer 150 mm high, i.e. the refining volume was 0.0696 m^3. The glass input and output were square openings having the side size 160 mm. The inner layer of the channel was formed by the corrundo-baddelleyite material (thickness 200 to 250 mm), the outer layer by the fireclay (thickness 200 mm). When modelling the fining channel, only parameters of the fining process have been considered, i.e. the size and shape of the channel, the presence or absence of the refining agent and the temperature-pressure conditions. The technical problems involving glass heating as well as input and output of glass from the reduced pressure were not included. In all calculations, the appropriate constant temperature was put on the glass level as the boundary condition. The glass model [5] was used to calculate the temperature and velocity fields of the glass melts in the channel and to get the pathways of bubbles. The appropriate values of bubble growth rates were taken from figures 2 and 3 in form of empirical dependencies between $(da/d\tau)_D$ and temperature under constant pressure. The initial radius of modelled bubbles was $5 \cdot 10^{-5}$ m.

When modelling the bubble pathways in the refining space, the bubble concentration model was applied [6],

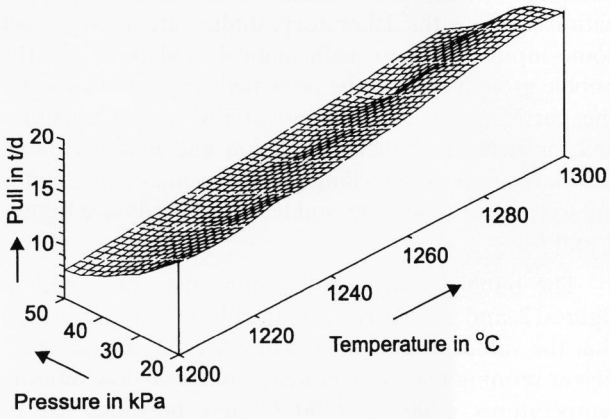

Figure 8. Pull rate of the modelled refining space as a function of temperature and pressure for the lead-silica glass melt with refining agent.

making it possible to acquire both bubble pathways and bubble concentrations in the space. In each experiment, 100 representative bubbles were distributed in the input opening to define the critical bubble pathway under given conditions. Figures 7a and b present an example of determination of the critical bubble pathway at 1200 °C and pressure 30 kPa for the glass melt with refining agent and the pull rate 10 t/d. The critical bubble is characterized by its refining just before the output of the space (the remaining bubbles are removed earlier). The average temperature along the critical bubble pathway and applied pressure characterize the overall conditions of refining in the space and consequently, the refining output of the low-pressure space. The dependences between calculated channel pull rate and temperature and pressure in the applicable area (see figures 5 and 6) are presented in figures 8 and 9.

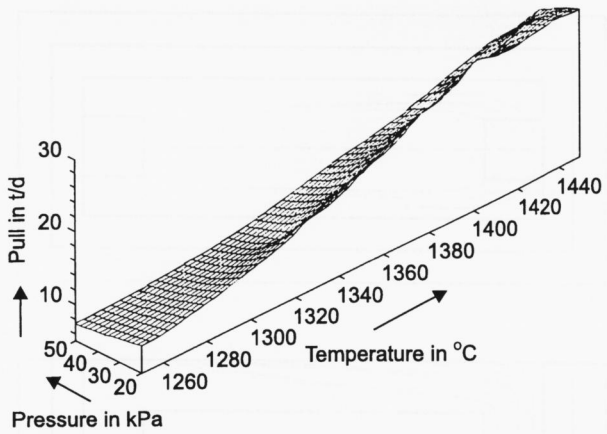

Figure 9. Pull rate of the modelled refining space as a function of temperature and pressure for the lead-silica glass melt without refining agent.

6. Discussion of results

The presented results show that the coupling of mathematical modelling and laboratory studies provides technologically acceptable conditions for industrial applications. While the laboratory studies are used to get some input data into mathematical models, as are the bubble growth rates in the presented case, and to specify the participation of other potentially critical phenomena, as here are bubble nucleation and glass foaming, the mathematical modelling provides values corresponding to the real conditions and technical needs (see figures 8 and 9).

The bubble growth and refining data presented in figures 2 and 3 confirm the already presented fact [1] that the values of bubble growth rates characterizing efficient refining may be acquired at relatively low refining temperatures 1200 to 1300 °C and pressures 20 to 30 kPa. The additional constraints evoked by bubble nucleation on the walls of the refining channel and by glass foaming restrict the entire temperature and pressure area of refining to 1200 to 1300 °C and 20 to 50 kPa for the lead glass melt containing refining agents and to 1250 to 1450 °C and 20 to 50 kPa for the same melt without any refining agents (see figures 5 and 6).

The estimation of refining behaviour based on the knowledge of several simple relations is significant when only a limited amount of experimental data is at disposal. The refining output of a horizontal channel with piston flow is given by:

$$\text{pull} = \frac{V\varrho}{\tau_R} \tag{7}$$

where V is the channel volume, ϱ is the glass density and τ_R is the refining time of the critical bubble.

For the efficient refining (growing bubble) and the sufficiently small critical bubble, the value of τ_R may be obtained from [7]:

$$\tau_R = \left(\frac{27\,h}{2g\varrho}\right)^{1/3} \frac{\eta^{1/3}}{\dot{a}^{2/3}} \tag{8}$$

where h is the height of glass in the channel, η the glass viscosity and $\dot{a}$ the constant value of bubble growth rate. As it is obvious from equation (8), the value of τ_R under the constant h exhibits a stronger dependence on the bubble growth rate when compared with glass viscosity.

The temperature increase accelerates bubble rising by both increasing the bubble growth rate and decreasing viscosity. The pressure drop, however, evokes only increase accrual of bubble growth rate. The separated impacts of temperature and pressure on the refining output are expressed by rectangular cuts through the output areas in figures 8 and 9. For the quiescent glass melt, the dependence between the refining time, τ_R, and temperature may be roughly expressed by [7]:

$$\tau_R = K_R^T \exp\left(\frac{E_R}{RT}\right) \tag{9}$$

where E_R involves the activation energy of diffusion, the reaction enthalpy of refining agent decomposition and activation energy of viscosity, and K_R^T is constant.

The pressure effect may be expressed by [7]:

$$\tau_R = \frac{p_{ex}^{2/3}}{(K_{R1}^p - K_{R2}^p p_{ex})^{2/3}} \tag{10}$$

where p_{ex} is the external pressure and K_{R1}^p as well as K_{R2}^p are constants.

As the results of calculations presented in figures 8 and 9 were not acquired at constant temperature, the following equations express the cuts through the output surfaces only qualitatively:

$$\text{pull}^T = \frac{V\varrho}{K_R^T} \exp\left(-\frac{E_R}{RT}\right), \tag{11}$$

$$\text{pull}^p = \frac{V\varrho}{p_{ex}^{2/3}} (K_{R1}^p - K_{R2}^p p_{ex}) . \tag{12}$$

If the appropriate experimental data characterizing the temperature and pressure impact are acquired, the preliminary assessments of the industrial refining efficiency may be done, using equations (11) and (12).

The significance of the temperature or pressure variances on the refining efficiency can be evaluated from the dependence between the pull rate of refining space and the bubble growth rate as the principal refining parameter. Figure 10 presents this dependence for the glass melt containing refining agent. The full line represents the dependence between the pull rate and pressure at temperature 1225 °C, the average value, on the pathway of the critical bubble. The dashed lines express the temperature dependencies of the pull rate at given pressures

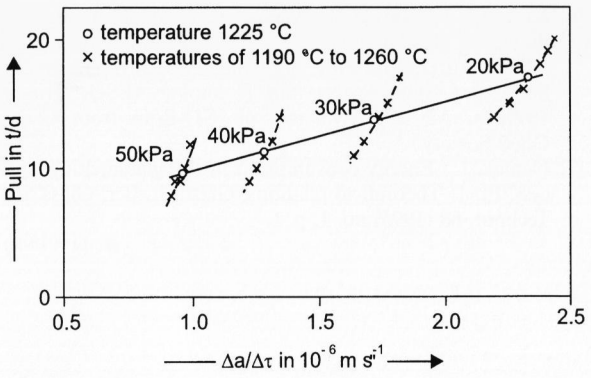

Figure 10. Pull rate of the modelled refining space as a function of the bubble growth rate for the lead-silica glass melt with refining agent; ———: pressure dependence at 1225 °C, – – –: temperature dependencies at the appropriate values of pressure.

Table 2. Values of E/R for the bubble growth rates in the studied lead-silica glass and soda-lime-silica glass melt (refined by sodium sulphate)

	E_η/R in K	E_a/R in K
lead-silica glass	20262	−4667[1)]
soda-lime-silica glass	22521	−60086

[1)] The value valid for the glass melt containing refining agents at pressure 20 kPa.

in the range 1225 °C ± 35 K. The dependence makes it possible to assess the participation of the particular quantities in the refining process. As it is obvious from figure 10, the temperature variance by ± 35 K has the same refining effect as the pressure variance ± 10 kPa. From the point of view of energy consumption, the pressure application is much more favourable under these conditions.

The difference between the pull rate values on the full line in figure 10 (pressure dependence) and dashed line (temperature dependence) at the same value of the bubble growth rate expresses the separated influence of viscosity variance on the refining pull. The relatively significant influence of the viscosity variance on the refining efficiency can be seen from this figure. This fact results from the relatively insignificant dependence between bubble growth rate and temperature (see figure 2). The participation of the viscosity change and bubble growth rate in the refining acceleration can be assessed from the appropriate activation energies. Table 2 provides the terms E/R involving the activation energy of viscosity, E_η, and apparent activation energy of the bubble growth rate, E_a, for the studied lead glass and soda-lime-silica glass. The latter glass is characterized by the steep temperature dependence of the bubble growth rate. The comparison between E_η/R and E_a/R for both glasses shows that in contrast to the studied lead glass, the impact of the bubble growth rate on the refining process acceleration is determining for the soda-lime-silica glass.

The presented results and considerations give the procedure leading to the proper industrial refining conditions: at first definition of admissible temperature and pressure areas without interference of other processes deteriorating glass quality or restricting the main process efficiency. The laboratory realization of this step seems to be more accessible at present. Equations (7 and 8) or (11 and 12) can help when estimating the mentioned temperature and pressure areas from the technical and economical point of view. The chosen areas should be subsequently submitted to the mathematical modelling under real conditions. The combined laboratory and theoretical modelling thus provides the technical documentation of the process character and parameters of industrial equipment.

7. Conclusion

The presented study aspires to combination of both laboratory data and mathematical modelling when determining the construction and conditions of an industrial refining space. The combined experimental and theoretical approach seems to be the most reliable at present as the complete mathematical models are mostly not at disposal. The laboratory studies are predominantly concentrated on the melting microphenomena (bubble behaviour, particle dissolution etc.), whereas the macrobehaviour is acquired from mathematical models (temperature and velocity distribution). Despite the fact that the micro- and macrophenomena mutually affect each other, their separate laboratory and mathematical treating mostly leads to acceptable predictions for an industrial case. As to the presented case, more detailed laboratory studies of glass foaming and bubble nucleation are needed in the future.

*

This work was supplied with a subvention by The Ministry of Education, Youth and Sports of the Czech Republic, project no. VS 96065.

8. References

[1] Němec, L.; Schill, P.; Chmelař, J.: Glass refining at reduced pressure. Glastech. Ber. **65** (1992), no. 5, p. 135–141.
[2] Takeshita, S.; Nakajima, S.; Tanaka, C. et al.: Refining of glasses under subatmospheric pressures. In: Proc. XVI International Congress on Glass, Madrid 1992. Vol. 6. p. 173–178. (Bol. Soc. Esp. Ceram. Vid. 31-C (1992) 6.)
[3] Kawaguchi, T.; Okada, M.; Ishimura, K. et al.: Refining of glasses under subatmospheric pressures. In: Proc. XVIIth International Congress on Glass, San Francisco 1998. Book of Abstracts , p. AB 121.
[4] Němec, L.; Kloužek, J.; Maryška, M. et al.: Visual observation and image analysis in the glass quality evaluation

and modelling of the glass melting process. In: Schaeffer, H. A.; Pye, L. D.: Proc. International Conference Advances in Fusion and Processing of Glass, May 22–24, 1995, Würzburg (Germany), p. 134–139. (Glastech. Ber. Glass Sci. Technol. 68 C2 (1995).)

[5] Chmelař, J.; Schill, P.; Franěk, A.: Mathematical models of glass melting furnaces. In: Schaeffer, H. A.; Pye, L. D.: Proc. 4th International Conference Advances in Fusion and Processing of Glass, Würzburg 1995. p. 63–66. (Glastech. Ber. Glass Sci. Technol. 68 C2 (1995).)

[6] Kloužek, J.; Matyáš, J.; Němec, L. et al.: Mathematical model of glass quality – bubble distribution in a glass melting furnace. In: Proc. 5th Conference of the European Society of Glass Science and Technology (ESG), Prague 1999, p. A2–25. (Available on CD-Rom from Czech Glass Society.)

[7] Němec, L.: Energy consumption in the glassmelting process. Pt. 1. Theoretical relations. Glastech. Ber. Glass Sci. Technol. **68** (1995) no. 1, p. 1.

1100P001

Addresses of the authors:

J. Kloužek, L. Němec
Laboratory of Inorganic Materials
Institute of Inorganic Chemistry ASCR and
Institute of Chemical Technology
Technická 5
166 28 Prague
Czech Republic

J. Ullrich
Glass Service Ltd.
Rokytnice 60
755 01 Vsetín
Czech Republic